Published in final edited form as:
Circ Cardiovasc Imaging. 2013 November ; 6(6): 1092–1101. doi:10.1161/CIRCIMAGING.113.000335.

Imaging for Pre-Intervention Planning: Pre and Post-Fontan Procedures

Mark A. Fogel, MD[a,b], **Reza H. Khiabani, PhD**[c], and **Ajit Yoganathan, PhD**[c]

[a]Division of Cardiology, Department of Pediatrics, The Children's Hospital of Philadelphia, The University of Pennsylvania School of Medicine, Philadelphia, PA 19104

[b]Department of Radiology, The Children's Hospital of Philadelphia, The University of Pennsylvania School of Medicine, Philadelphia, PA 19104

[c]The Wallace H. Coulter Department of Biomedical Engineering, Georgia Institute of Technology & Emory University, Atlanta, GA 30332

Introduction

Although all preoperative imaging can be considered “surgical planning” (SP), it will be defined in this article as the act of utilizing preoperative data to simulate the surgical procedure or the result of the procedure. It is the combination, all or in part, of 3-dimensional (3D) medical imaging, applied computer vision, computer-aided design and computational fluid dynamic modeling (CFD) to mimic and/or provide visual guidance for surgical procedures. This simulation is generally performed with multiple anatomic and physiologic states to determine the robustness of the procedure. There are multiple advantages to this approach such as assessing standard interventions and creation of new surgical strategies without risking the patient’s health; this can potentially have both clinical and economic benefit.

Since its first mention almost 30 years ago, SP is now a routine part of interventions in fields such as neurosurgery and orthopedics.[1] Translating this paradigm to cardiovascular interventions not only provides enhanced 3D visualization, but also the potential to interface with physics-driven computational solvers (e.g., CFD) to predict the hemodynamic outcomes. Considering the complexity of fluid-solid interactions and the highly time-varying component of the cardiovascular system, these efforts are largely lagging behind those in the neurological and orthopedic communities, but recent advances appear promising. [2]

The Fontan operation for single ventricle (SV) patients, where a conduit (the total cavopulmonary connection [TCPC]) is placed to channel systemic venous return passively into the pulmonary arteries, is the paradigm for this approach. This category of lesions is the leading cause of morbidity and mortality in congenital heart disease and although it is generally associated with acceptable short-term outcomes, “Fontan failure” remains a problem. Progressive ventricular dysfunction, protein-losing enteropathy, poor exercise tolerance, pulmonary arteriovenous malformations (PAVM), and liver dysfunction are some

Correspondence to: Mark A. Fogel, MD, FACC, FAHA, FAAP, The Children's Hospital of Philadelphia, Division of Cardiology, 34th St. and Civic Center Blvd., Philadelphia, PA 19104, Telephone: 215-590-7566, Fax: 215-590-5825, fogel@email.chop.edu.

Disclosures

Dr. Fogel has a grant from Edwards Life Sciences and Siemens Medical Solutions and is medical monitor for an imaging agent from Kereos. Dr. Yoganthan has no disclosures.

of the most commonly cited complications. These morbidities are multi-factorial and the underlying causes in many cases are unknown, however, there is mounting evidence suggesting that TCPC hemodynamics play an important role in their development. For example, exercise intolerance may be related to non-linear increases in TCPC power loss (PL) with increasing exercise level, which contributes substantially to ventricular preload limitations.[3,4] The SP approach can yield clues to these complications and potentially avoid them by simulating the multiple TCPC geometries and hemodynamics in a "patient specific" fashion to determine the optimal design.

There are 2 main goals to date of SP in the SV patient. One is to minimize the PL in the Fontan baffle (systemic venous pathway). As mentioned, this allows passive flow of blood from the systemic venous return to enter the lungs without the use of a pumping ventricle. Because of this, minimizing the PL at this level is very important to allow for easier transit of blood into the lungs. A second goal is to distribute an equal amount of hepatic blood flow to both lungs. It is known that some form of an unidentified "hepatic factor" (HF) inhibits the formation of pulmonary arterio-venous malformation (PAVM) (ie lack of this factor produces PAVMs); in lungs with PAVMs, introduction of hepatic blood flow (and with it, the "hepatic factor") will cause the PAVM to regress. Certain types of SV patients are a setup for a lack of HF (bidirectional Glenn patients, heterotaxy patients) so it is clear that a benefit would accrue if SP could design baffles to maintain hepatic factor levels to both lungs (see below). These 2 goals are amenable to SP as the geometry of the Fontan baffle can be altered to minimize energy loss and direct blood appropriately.

The Surgical Planning Approach

The overall SP procedure as it relates to the Fontan operation and the TCPC is summarized in figure 1 top and contains 4 basic steps with 2 assessment stages. Preoperative imaging is obtained using cardiac magnetic resonance (CMR) for anatomy and flows followed by detailed image processing to determine the current hemodynamics and physiology. "Virtual surgery" is performed on a workstation in conjunction with bioengineers, cardiologists and surgeons to determine various options with CFD subsequently performed to obtain the physiology and hemodynamics of each option. Finally, the team meets to determine which option is optimal and then surgery is performed.

The SP approach that the authors developed requires patient-specific anatomy. Although static steady state free precession (SSFP) CMR is the method presented, the reconstruction tools can be applied to different types of CMR (eg angiography) and imaging modalities (eg computed tomography), as long as they provide enough anatomical details for segmentation. The following is more detail on each phase of the process.

1. *CMR:* The minimum imaging required as input for the current process consists of:
    - high resolution stack of cardiac-gated, static axial steady SSFP images to reconstruct the bidirectional Glenn or TCPC and surrounding structures; this can be done with or without T2 preparation (eg whole heart imaging). Angiography was not optimal since it is not cardiac gated and the borders of the cardiovascular structures tend to be blurred.
    - Through-plane retrospectively gated, phase-encoded velocity maps (PCMR) across all vessels of interest including all cavae, the TCPC immediately inferior to the branch pulmonary arteries (to account for fenestration flow), hepatic veins if needed and across the branch pulmonary arteries (PAs) at a minimum. In addition, PCMR is performed across the aortic root, the main pulmonary artery (if present), the pulmonary veins and the descending aorta at the level of the diaphragm.

- Optional imaging includes 4-dimensional flow stack in the coronal plane across the TCPC to determine the in-vivo flows and to compare with the calculated CFD flows which will subsequently be generated.

2. *Anatomic reconstruction:* Our group has previously developed and extensively utilized techniques[5,6] (figure 1 bottom) to accurately reconstruct patient anatomy from CMR images which include : 1) Interpolation, which ensures isotropic sizing for each volume element of the stack, 2) Segmentation, which can handle incomplete vessel edge definitions, and 3) 3D Reconstruction, which defines a smooth and coherent 3D surface from the segmented stack. Analysis of PCMR data (Velocity segmentation): This methodology employs parametric active contours with Gradient Vector Flow,[7] in which the user specifies an initial contour that evolves under the influence of internal and external energy fields to precisely sit on the vessel border. Flow artifacts and noise are eliminated with an automatic, adaptive median filtering approach. Validation against manual segmentation demonstrated an excellent agreement between the two methods with less than 1% difference in resulting flow rates.[8].

3. *CFD:* By numerically solving the basic fluid mechanics (Navier-Stokes equations) and mass conservation equations, CFD methods provide flow and pressure fields in a physical domain for given boundary conditions.[9] CFD solver software especially tailored to address the complexities and challenges of modeling the cardiovascular system is used to simulate transient, internal flows in arbitrarily complex shapes, such as TCPC anatomies. Through numerous experimental test cases, the time averaged velocity fields and flow profiles have had excellent agreement with both experimental and in vivo imaging data.[10] Control volume PL and hepatic flow distribution (HFD) are the primary end points from these simulations and is used to evaluate and discriminate between surgical options.

4. *Virtual Surgery:* After the anatomy and PCMR data is analyzed, CFD is utilized to determine the current physiology and hemodynamics. Detailed discussions among bioengineers, cardiologists and surgeons occur to determine the best surgical options to test.

   A major milestone for the systematic investigation of alternate Fontan surgical procedures is the ability to modify the pre-operative anatomy to model different post-operative configurations. To this end, our group has developed a robust and practical interface that reproduces surgical motions (SURGEM) via two free-form haptic devices which is used to perform this procedure.

   Finally, an assessment of all options are done by bioengineers, cardiologists and surgeons and the best option is implemented.

5. *Lumped Parameter and Compliance Modeling:* Lumped parameter models are a widely-used tool for simulating the cardiovascular system. By exploiting analogies between fluid flow and electrical circuits, systemic responses can be assessed at a global level combining simplified models for each relevant section of the cardiovascular system without the need to model anatomic detail. Recently, such reduced order models have been combined with 3D CFD solvers as a means to improve the accuracy and realism of the prescribed boundary conditions.[11] This coupling strategy can be a particularly valuable tool to naturally approximate the post-operative flow conditions needed to properly evaluate the various surgical options, given the complex hemodynamic changes that occur following Fontan surgery. This is a useful aid.

The Beginnings of SP in Fontan Patients

One of the first attempts at using this approach in Fontan patients was fairly elementary; performing "virtual angioplasty" on a stenotic left pulmonary artery (LPA).[12] Pekkan et al. noted that in a large cohort of SV patients, 35% had significant narrowing of the LPA due to the large patulous aortic reconstructions and hypothesized that relief of this obstruction would significantly improve hemodynamics and PL. By utilizing CFD and modifying the geometry with specialized software, they found that not only did left lung perfusion increase (with no surprise) but that PL decreased with decreasing severity of the stenosis; this effect was more pronounced with diffuse stenosis than discrete stenosis. There were very high power losses (30 mW) with an 85% stenosis which were cut in half with virtual angioplasty to no narrowing. Adding a fenestration decreased the TCPC pressure but also decreased both left and right lung perfusion as well as increased hemodynamic PL.

This was followed up by another study where the Fontan baffle was actually moved in a case of bilateral superior vena cavae both connected to the ipsilateral PA. (figures 2 A and B)[13] In that report, the inferior vena cava (IVC) baffle was connected to the right superior vena cava (RSVC) - right pulmonary artery (RPA) anastomosis; although there were smooth and steady flow fields in other portions of the systemic venous pathway, flow disturbances and collisions were found at the RSVC-RPA connection with baffle flow. Left superior vena cava flow (LSVC) preferentially streamed to the LPA with the central pulmonary arteries being perfused by flow from the IVC and RSVC. When simulations were run with < 50% of the cardiac output streaming to the LPA, little flow was noted in the central pulmonary arteries which would be a setup for thrombus (flow stasis) and left PAVMs because of lack of HF (see below). By modifying the anatomy and shifting the baffle to the central pulmonary artery, not only was power loss decreased by 7% but no flow stasis was observed in the central pulmonary artery and a substantial amount of IVC blood (and HF) coursed to both lungs. Although not mentioned in this study, CFD modeling would be able to determine the optimal degree of angulation of the Fontan baffle if it was not anatomically possible to place it directly in the central pulmonary artery or determine the offset to one branch pulmonary artery in situations where there was unequal distribution of blood flow.

SP and PAVMs – Tackling A Difficult Problem

By definition, PAVMs are a complex tangled web of abnormal arteries and veins connected by > 1 fistulae in the lung bypassing the alveoli (no capillary bed of its own). One obvious problem this creates is cyanosis since bypassing the alveoli prevents gas exchange. In addition, the fistulae are a low resistance circuit, drawing blood away from the normal regions of the lung where gas exchange can occur to regions of the lungs where it can't, creating another dimension to the problem. As mentioned above, an unidentified "hepatic factor" can prevent these PAVMs from occurring although VEGF and nitric oxide as well as other vasoactive substances are also thought of to play a role.

It is estimated that 3% of single ventricle patients after bidirectional Glenn have PAVMs[14] and can develop rapidly, although they can resolve just as rapidly after completion of the Fontan procedure, presumably due to delivery of HF to the lungs.[15] Lending credence to the notion of HF is a report by AboulHosn et al. where PAVMs were found in lungs of Fontan patients with discontinuous branch PAs whose blood flow as soley from the SVC; after reconnection, the PAVMs regressed.[16]

Single ventricle patients with heterotaxy, specifically those with interrupted IVC with azygous continuation to an SVC, are especially susceptible to PAVM development. In these individuals, because the hepatic veins enter the right atrium directly, a Kawashima operation (ie a bidirectional Glenn procedure in this setting) directs all blood from the lower and upper

body to the pulmonary arteries except hepatic blood. Therefore, to baffle this blood into the lungs and complete the Fontan operation, a conduit or baffle must be created. Because hepatic venous flow is only 20–25% of the cardiac output, the challenge becomes creating a baffle in such a fashion to distribute hepatic flow equally to both lungs. A baffle too close to one branch PA may stream hepatic blood to that lung, causing the contralateral lung to develop PAVMs. This becomes an even more complex decision when there are bilateral SVCs, each one connected to the ipsilateral branch PA.

The first article describing SP to redirect hepatic venous flow to allow PAVMs to regress was published in 2009 by Sundareswaran et al.[17] In that case report, a SV patient with heterotaxy, dextrocardia and interrupted IVC with azygous continuation to the RSVC who was after a Kawashima operation and hepatic extracardiac conduit to the RPA was noted to have a systemic saturation of 72%. During catheterization, severe left PAVMs were noted and the patient underwent CMR and SP. The native anatomy and flow structure (figures 3 A and B) demonstrated vortex formation in a pouch formed by the SVC-RPA connection, blocking hepatic flow from the baffle to enter the LPA and causing streaming of this blood into the RPA (figure 3B, left column, arrow). The LPA received 70% of the cardiac output, however, the calculated hepatic flow to the LPA was low (~5%).

SP strategies included either increasing hepatic flow kinetic energy (unlikely), avoiding head-on collision of hepatic flow with the vortex or disrupting the vortex entirely. After long and lengthy discussions, options which were considered included a “Y” graft from hepatic veins which straddled the pouch, connecting the azygous to the hepatic conduit and connecting the hepatic conduit to the azygous (figures 3A and B). The final option noted, connection of the hepatic conduit to the azygous, demonstrated the best performance with a 66/34% LPA/RPA split of hepatic flow, close to the global flow distribution of 70/30% (figure 3B, right column). This option was performed and at the 5 month followup, the systemic saturation was 94% with presumed resolution of the PAVMs.

De Zelicourt et al. described our experience utilizing SP with 5 single ventricle patients with interrupted IVC and severe PAVMs in an attempt to channel hepatic blood to both lungs equally.[2] By using CMR for flows and anatomy, global and hepatic flow distributions along with PL were calculated in the current physiologic setup and virtual surgeries were performed to determine the optimal configuration of the hepatic baffle. Because of the low flow rate of hepatic blood, the conduit is very sensitive to the offset with the SVC where nearly the entire cardiac output returns to the PAs; even a small offset can lead to a highly asymmetrical hepatic flow distribution. In the 3 patients with a single SVC, because of this fact, the best approach appeared to be a “Y” graft straddling the SVC-PA connection or a hepatic conduit to azygous connection. In patients with bilateral SVCs, the best approach appeared to be connecting the baffle to the central pulmonary artery in between the 2 SVCs.

Proof of concept is further enhanced by the prediction of development of PAVMs. Figures 4 demonstrates data from a 6 year old male with single ventricle, bilateral SVCs, interrupted IVC with azygous continuation to an LSVC who was after a Kawashima operation and hepatic baffle connection to the RSVC-RPA junction. There was significant central pulmonary artery stenosis and no evidence for PAVMs. The patient was referred for CMR and CFD modeling to determine the amount of hepatic flow to each lung and results demonstrated that <10% was coursing to the left lung, implying that this lung was at risk for PAVM development. Two years later, the patient’s systemic oxygen saturation had dropped from the mid 90s to the low 80s and cardiac catheterization revealed significant left lung PAVMs. A repeat CMR and CFD study done at that time demonstrated <1% hepatic flow coursing to the left lung.

Beyond PAVMs

SP has other applications in the single ventricle patient, such as in the "routine" Fontan. Figure 5 are CMR images from a nearly 3 yo with heterotaxy, dextrocardia, single ventricle patient with infradiaphragmatic total anomalous pulmonary venous connections, midline liver after bilateral bidirectional Glenn and pulmonary vein repair. As can be seen, the left hepatic veins entered separately (on the left side of the atrial septum) from the IVC and right hepatic veins (right side of the atrial septum) so connecting these together presented a challenge. In addition, the pulmonary veins and pulmonary venous confluence appear to be in the path of a number of possible Fontan conduits. Figures 6 A and B are 8 possible scenarios explored anatomically and with flow structures respectively including a conduit coursing up the left side of the cardiac mass. One option (a), where a separate conduit for the left hepatic veins and the IVC-right hepatic veins, was thought impractical due to low flow in the left conduit and the risk of thrombosis (orange arrow). All other geometries except (b) had flow disturbances thought to be less than optimal (red arrows). Figure 6C is the quantitative data for hepatic flow distribution and PL demonstrating that (b) was the best option as well.

SP can also be utilized to evaluate new and novel conduit designs. For example, a study published in 2007 proposed the "Optiflow" design for the systemic venous pathway.[18] In that proposal, the SVC and Fontan conduit connections to the branch pulmonary artery was suggested to be a diamond shape configuration. (figure 7); this allowed for lower PL (with the exception of low flow 2 liters/minute) in the systemic venous pathway relative to a standard Fontan at all flow splits to the RPA. As this may not be practical in some cases, a "Y" graft was also proposed and evaluated (figure 7); this was found to also have better PL and flow structures than the standard Fontan. This was followed by a study by Marsden et al.[19] who also proposed 2 "Y" graft variants – "off the shelf" and "area preserving" designs - which was evaluated at rest and at exercise; they found that the "area preserving" graft had greater efficiency than the other in both conditions, decreased caval pressures at exercise and better distributed inferior vena cava flow. In 2012, that same group demonstrated that HF was better distributed by the "Y" design than either the classic "T" junction or an offset of the baffle from the SVC.[20] Multiscale lumped parameter models of these designs have also been performed.[21]

Smoke and Mirrors?

The images are appealing and SP appears useful clinically, but do the flow structures and hemodynamics have any basis in reality or is this just smoke and mirrors? We answered that question in 3 different ways, all of which demonstrate that CFD and SP faithfully describe what occurs in vivo:

1. A qualitative comparison of the flow structure between angiography and what CFD predicts (figure 8A)
2. Comparison between the flow structure in vivo as directly measured by 4-dimensional flow imaging and what CFD predicts (figure 8B, left).
3. Quantitative comparison between CFD flow structure in SP designed Fontan conduits and the superimposition of the pre-operative boundary conditions (flows at the inlets and outlets) on the post-operative anatomy the surgeon actually created; the resultant flows were very close to each other (figure 8B, right).

Implications and Conclusion

The use of SP in designing, redesigning and building a better Fontan utilizes CMR for anatomy and flows along with CFD and advanced bioengineering and computing

environments. It has been used successfully and most extensively in single ventricle patients with PAVMs to direct hepatic blood flow evenly to both lungs as well as predicting PAVMs, however, it is currently being extended to the routine Fontan patient along with testing out and designing more optimized Fontan geometries. More work is definitely needed to refine the process to make it more robust, quicker and easier; at the moment, very few centers are capable of this technology. In the future, SP will most likely be extended to other surgical lesions. SP holds the promise of truly individualized medicine and surgery, optimizing surgical outcome virtually and therefore minimizing the risk to the patient.

Acknowledgments

Sources of Funding

This work was partially funded by 2 NIH grants: The Bioengineering Research Partnership R01 HL67622-01 and R01HL098252-01.

References

1. Vannier M, Marsh J. Three dimensional ct reconstruction images for craniofacial surgical planning and evaluation. Radiology. 1984; 150:179–184. [PubMed: 6689758]
2. de Zélicourt DA, Haggerty CM, Sundareswaran KS, Whited BS, Rossignac JR, Kanter KR, Gaynor JW, Spray TL, Sotiropoulos F, Fogel MA, Yoganathan AP. Individualized Computer-Based Surgical Planning To Address Pulmonary Arteriovenous Malformations in Patients With A Single-Ventricle With An Interrupted Inferior Vena Cava and Azygous Continuation. J Thorac Cardiovasc Surgery. 2011; 141:1170–1177.
3. Whitehead KK, Pekkan K, Kitajima HD, Paridon SM, Yoganathan AP, Fogel MA. Nonlinear power loss during exercise in single-ventricle patients after the fontan: Insights from computational fluid dynamics. Circulation. 2007; 116:I165–I171. [PubMed: 17846299]
4. Sundareswaran KS, Pekkan K, Dasi LP, Whitehead K, Sharma S, Kanter K, Fogel M, Yoganathan AP. The total cavopulmonary connection resistance: A significant impact on single ventricle hemodynamics at rest and exercise. American Journal of Physiology Heart and Circulatory Physiology. 2008; 295:H2427–H2435. [PubMed: 18931028]
5. Frakes DH, Smith MJ, Parks J, Sharma S, Fogel SM, Yoganathan AP. New techniques for the reconstruction of complex vascular anatomies from mri images. J Cardiovasc Magn Reson. 2005; 7:425–432. [PubMed: 15881525]
6. de Zelicourt D, Pekkan K, Wills L, Kanter K, Forbess J, Sharma S, Fogel M, Yoganathan AP. In vitro flow analysis of a patient-specific intraatrial total cavopulmonary connection. Annals of Thoracic Surgery. 2005; 79:2094–2102. [PubMed: 15919316]
7. Frakes D, Smith M, Zelicourt Dd, Pekkan K, Yoganathan AP. Three-dimensional velocitiy field reconstruction. Journal of Biomechanical Engineering. 2004; 126:727–735. [PubMed: 15796331]
8. Sundareswaran K, Frakes D, Fogel M, Soerensen D, Oshinski JN, Yoganathan A. Optimum fuzzy filters for phase-contrast magnetic resonance imaging segmentation. Journal of Magnetic Resonance Imaging. 2009; 29:155–165. [PubMed: 19097101]
9. Pekkan K, de Zelicourt D, Ge L, Sotiropoulos F, Frakes D, Fogel M, Yoganathan AP. Physics-driven cfd modeling of complex anatomical cardiovascular flows- a tcpc case study. Annals of Biomedical Engineering. 2005; 33:284–300. [PubMed: 15868719]
10. Tang E, Haggerty C, Khiabani R, de Zelicourt D, Kanter J, Sotiropoulos F, Fogel M, Yoganathan A. Numerical and experimental investigation of pulsatile hemodynamics in the total cavopulmonary connection. Journal of Biomechanics. 2013; 46:373–382. [PubMed: 23200904]
11. Pennati G, Corsini C, Cosentino D, Hsia T-Y, Luisi VS, Dubini G, Migliavacca F. Boundary conditions of patient-specific fluid dynamics modelling of cavopulmonary connections: Possible adaptation of pulmonary resistances results is a critical issue for virtual surgical planning. Interface Focus. 2011; 1:297–307. [PubMed: 22670201]
12. Pekkan K, Kitajima HD, de Zelicourt D, Forbess J, Parks JM, Fogel M, Sharma S, Kanter K, Frakes D, Yoganathan AP. Total Cavopulmonary Connection Flow with Functional Left

Pulmonary Artery Stenosis –Angioplasty and Fenestration in Vitro. Circulation. 2005; 112:3264–3271. [PubMed: 16286590]

13. de Zélicourt D, Pekkan K, Parks J, Kanter K, Fogel M, Yoganathan AP. Flow Study of an Extra-Cardiac Connection with Persistent Left Superior Vena Cava. J Thorac Cardiovasc Surg. 2006; 131:75–791.
14. Mahle WT, Rychik J, Rome JJ. Clinical significance of pulmonary arteriovenous malformations after staging bidirectional cavopulmonary connection. Am J Cardiol. 2000; 86:239–241. [PubMed: 10913495]
15. Shah MJ, Rychik J, Fogel MA, Murphy JD, Jacobs ML. Pulmonary AV malformations after superior cavopulmonary connection: Resolution after inclusion of hepatic veins in the pulmonary circulation. Ann Thorac Surg. 1997; 63:960–963. [PubMed: 9124971]
16. AboulHosn J, Danon S, Levi D, Castellon Y, Child J, Moore J. Regression of pulmonary arteriovenous malformations after transcatheter reconnection of the pulmonary arteries in patients with unidirectional Fontan. Congenit Heart Dis. 2007; 2:170–184. [PubMed: 18377461]
17. Sundareswaran KS, de Zelicourt D, Sharma S, Kanter KR, Spray TL, Rossignac J, Sotiropoulos F, Fogel MA, Yoganathan AP. Correction of pulmonary arteriovenous malformation using image-based surgical planning. J Am Coll Cardiol Img. 2009; 2:1024–1030.
18. Soerensen D, Pekkan K, de Zélicourt D, Parks J, Kanter K, Fogel M, Yoganathan AP. Introduction of a New Optimized Total Cavopulmonary Connection. Annals of Thoracic Surgery. 2007; 83:2182–2190. [PubMed: 17532420]
19. Marden AL, Bernstein AJ, Reddy M, Shadden SC, Spilker RL, Chan FP, Taylor CA, Feinstein JA. Evaluation of a novel Y-shaped extracardiac Fontan baffle using computational fluid dynamics. J Thorac Cardiovasc Surg. 2009; 137:394–403. [PubMed: 19185159]
20. Yang W, Vignon-Clementel IE, Troianowski G, Reddy VM, Feinstein JA, Marsden AL. Hepatic blood flow distribution and performance in conventional and novel Y-graft Fontan geometries: a case series computational fluid dynamics study. J Thorac Cardiovasc Surg. 2012; 143:1086–1097. [PubMed: 21962841]
21. Baretta A, Corsini C, Yang W, Vignon-Clementel IE, Marsden AL, Feinstein JA, Hsia TY, Dubini G, Migliavacca F, Pennati G. Modeling of Congenital Hearts Alliance (MOCHA) Investigators. Virtual surgeries in patients with congenital heart disease: a multi-scale modelling test case. Phil Trans R Soc A. 2011; 369:4316–4330. [PubMed: 21969678]

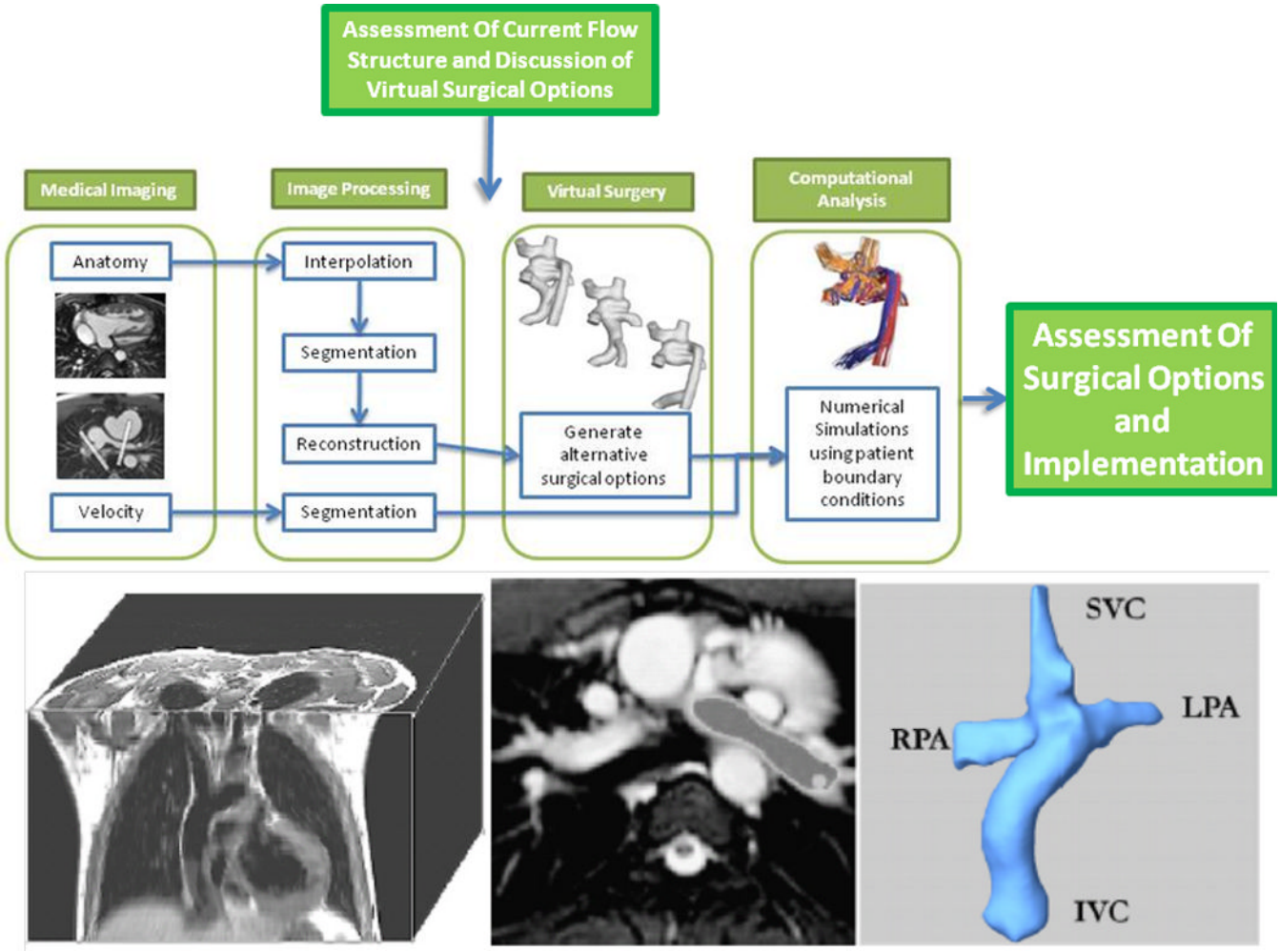

Figure 1.
(Top) Stages in the work flow in performing surgical planning. (Bottom) Creation of 3D geometry

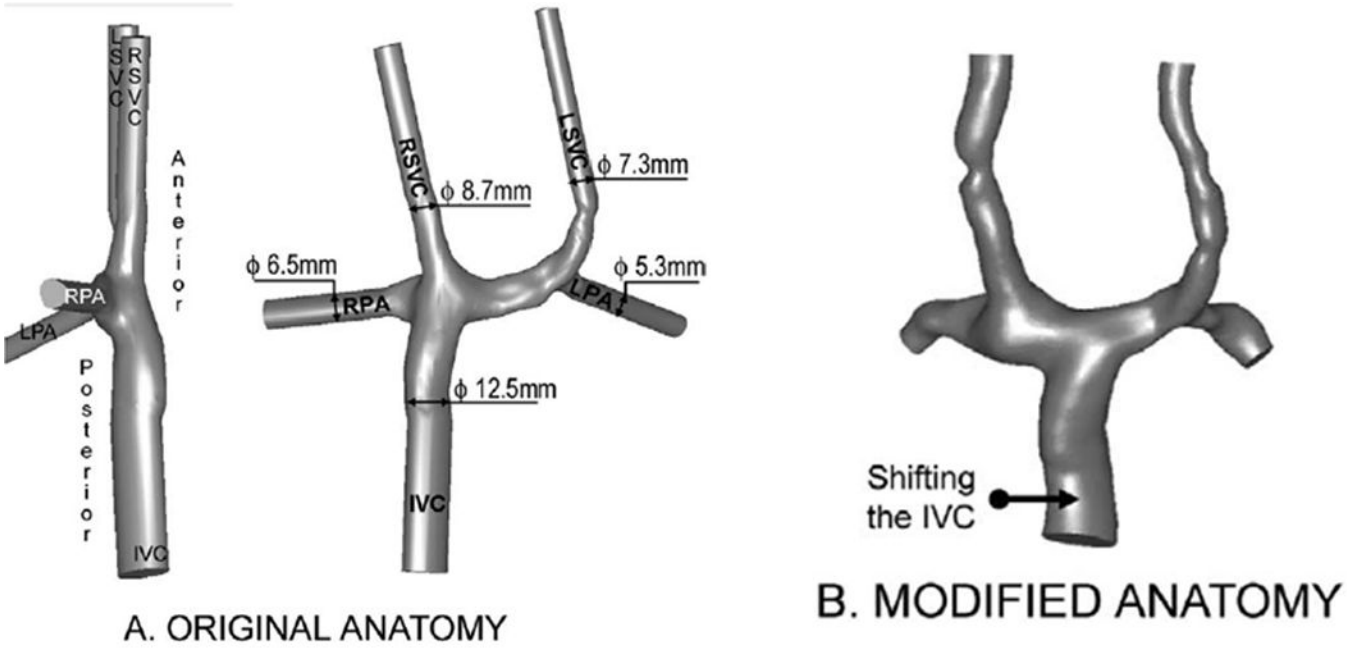

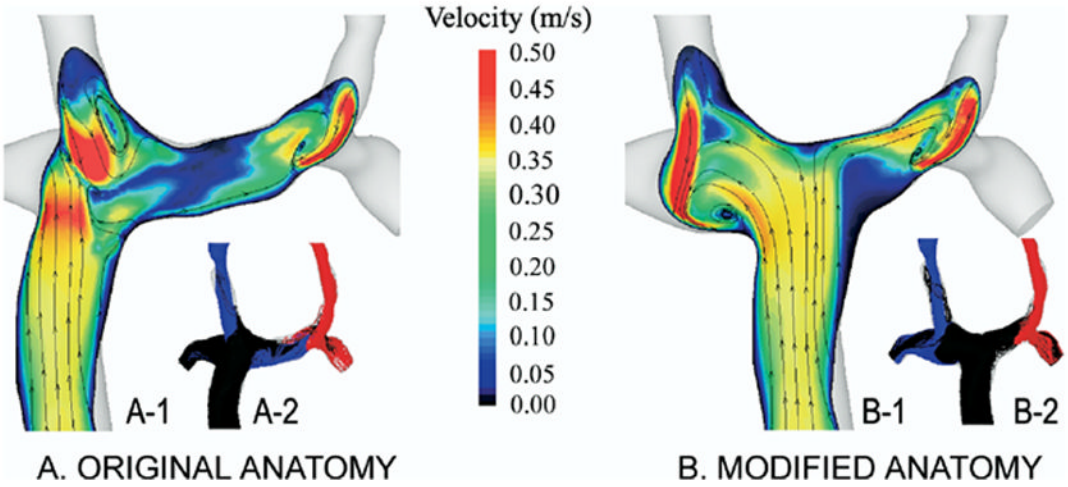

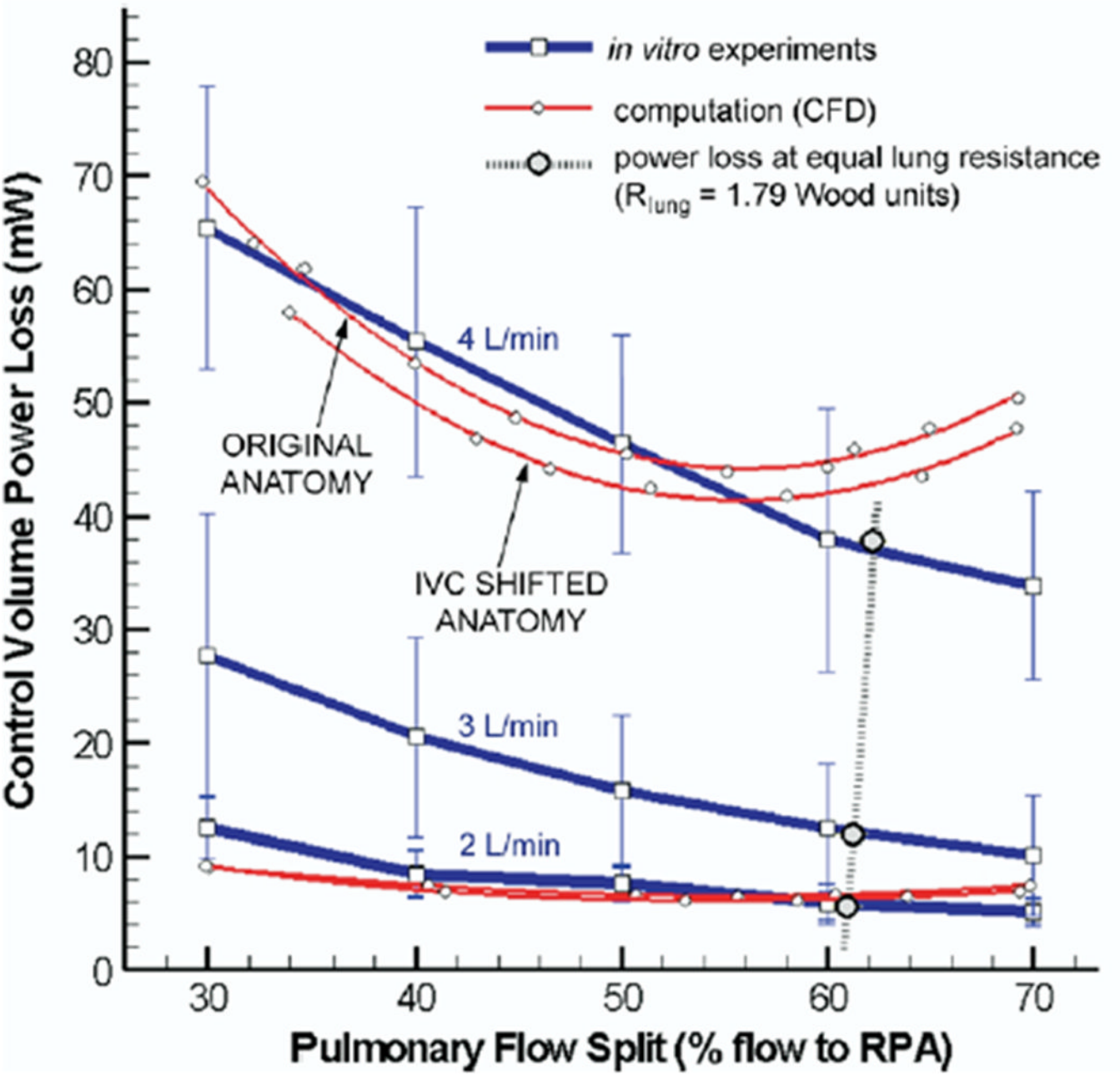

Figure 2.

Surgical planning utilized in a bilateral bidirectional Glenn/Fontan patient. (A). (Top) Original anatomy of the Fontan baffle and bilateral bidirectional Glenn connection is on the left; note the Fontan baffle is directly below the right superior vena cava (RSVC). On the right, the baffle is moved by "virtual surgery." (Bottom) Velocities as calculated by CFD in the original anatomy (left) and by virtual surgery (right). Note the low velocities in the central pulmonary artery in the original anatomy. (B). Graph of power loss on the Y axis and percent flow to the right pulmonary artery (RPA) on the X axis for the original anatomy and the virtual surgery (inferior vena cava, IVC shifted anatomy) for in-vitro flow experiments (blue line) and CFD (red lines) at 3 different flow rates. Note at 4 l/min where the comparison was performed, the virtual surgery anatomy performs better than the original

anatomy with lower PL. Note that the in-vitro measurements and CFD differ at that flow because of instabilities (Reynold's number > 2299 in the RPA at 70:30 RPA/LPA), reaching the limitations of the commercial CFD package used. LSVC=superior vena cava, LPA=left pulmonary artery, m/s=meters per second. From de Zélicourt D, Pekkan K, Parks J, Kanter K, Fogel M, Yoganathan AP. Flow Study of an Extra-Cardiac Connection with Persistent Left Superior Vena Cava. J Thorac Cardiovasc Surg. 2006;131:75–791. With permission.

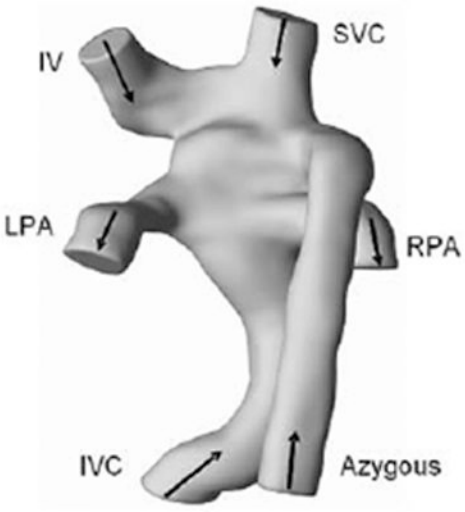

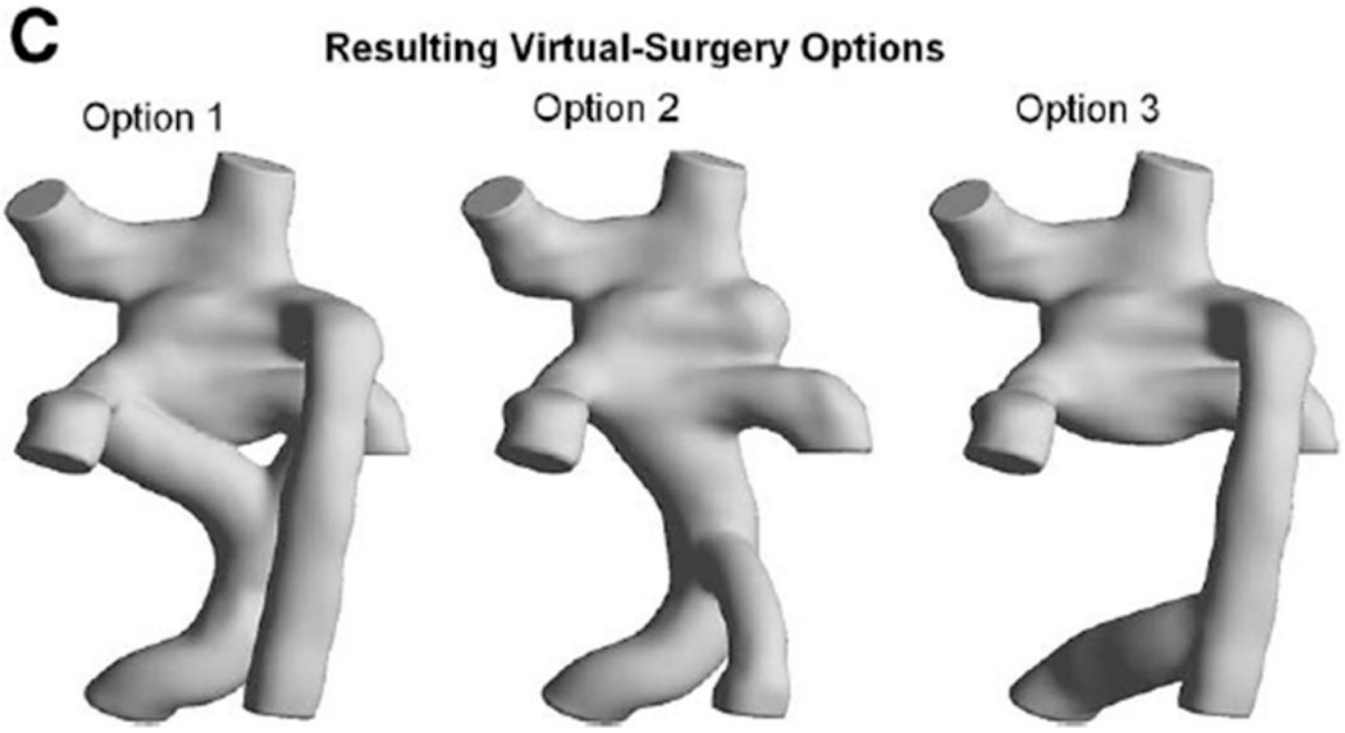

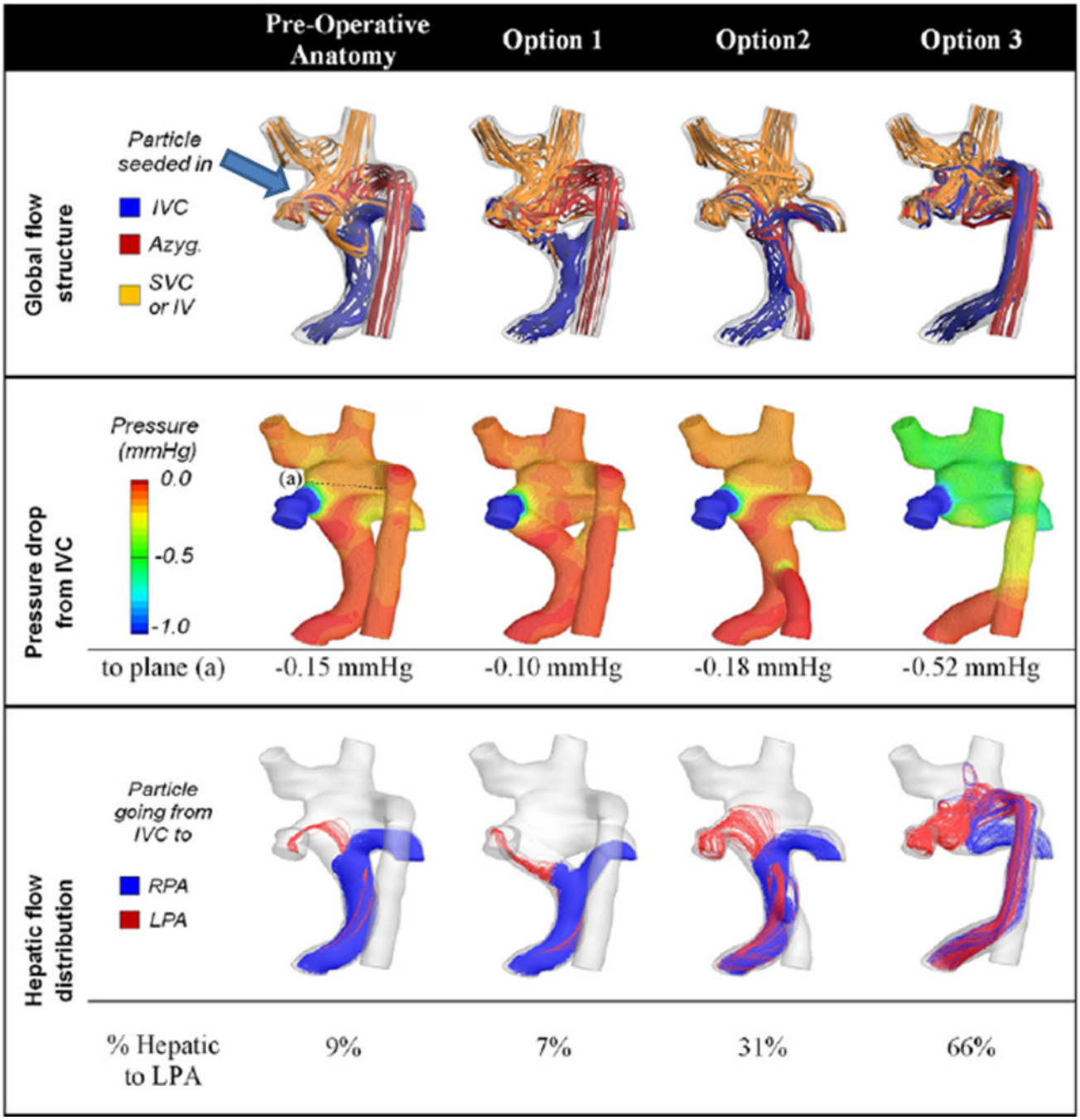

Figure 3.

Surgical planning in a Fontan patient with heterotaxy. (A) All 3D images are viewed from posterior. Original anatomy is at the top and the 3 virtual surgical options are at the bottom below the letter "C." Y graft, azygous connection to the hepatic baffle and hepatic baffle connection to the azygous are shown from left to right respectively. (B) Flow structures (top row), pressure drop (middle row) and hepatic flow (bottom row) for the original anatomy (left column) and the 3 surgical options are shown. Arrow points to the vortex formation in the original anatomy. Azyg=azygous, IV=innominate vein, IVC=inferior vena cava, LPA=left pulmonary artery, mm Hg= millimeters of mercury, RPA=right pulmonary artery, SVC=superior vena cava. From Sundareswaran KS, de Zelicourt D, Sharma S, Kanter KR,

Spray TL, Rossignac J, Sotiropoulos F, Fogel MA, Yoganathan AP. Correction of pulmonary arteriovenous malformation using image-based surgical planning. *J Am Coll Cardiol Img.* 2009;2:1024–1030. With permission.

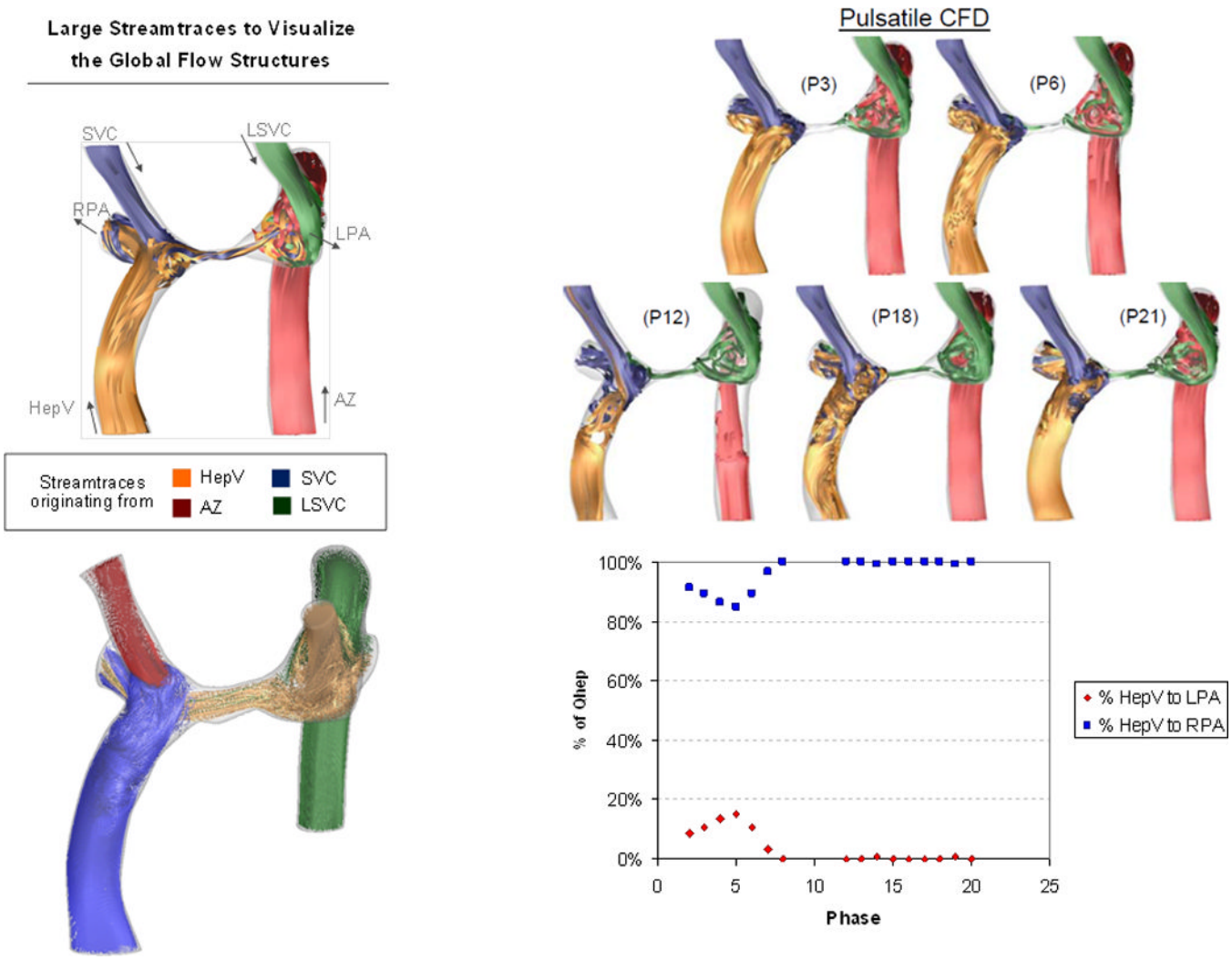

Figure 4.

Prediction of PAVMs in a heterotaxy patient. Time averaged flow structures in the original CMR (upper left) and at different phases of the cardiac cycle (upper right panel) with P being the phase and the following number being the phase. Lower right panel is the percent of hepatic blood vs phase graph, noting that little flow goes to the right pulmonary artery (RPA). Lower left panel is the global flow structure at the second CMR with hepatic vein flow (HepV) blue, right superior vena cava (SVC) flow red, left superior vena cava flow (LSVC) gold and azygous (Az) flow green. Note different color maps for the upper left panel.

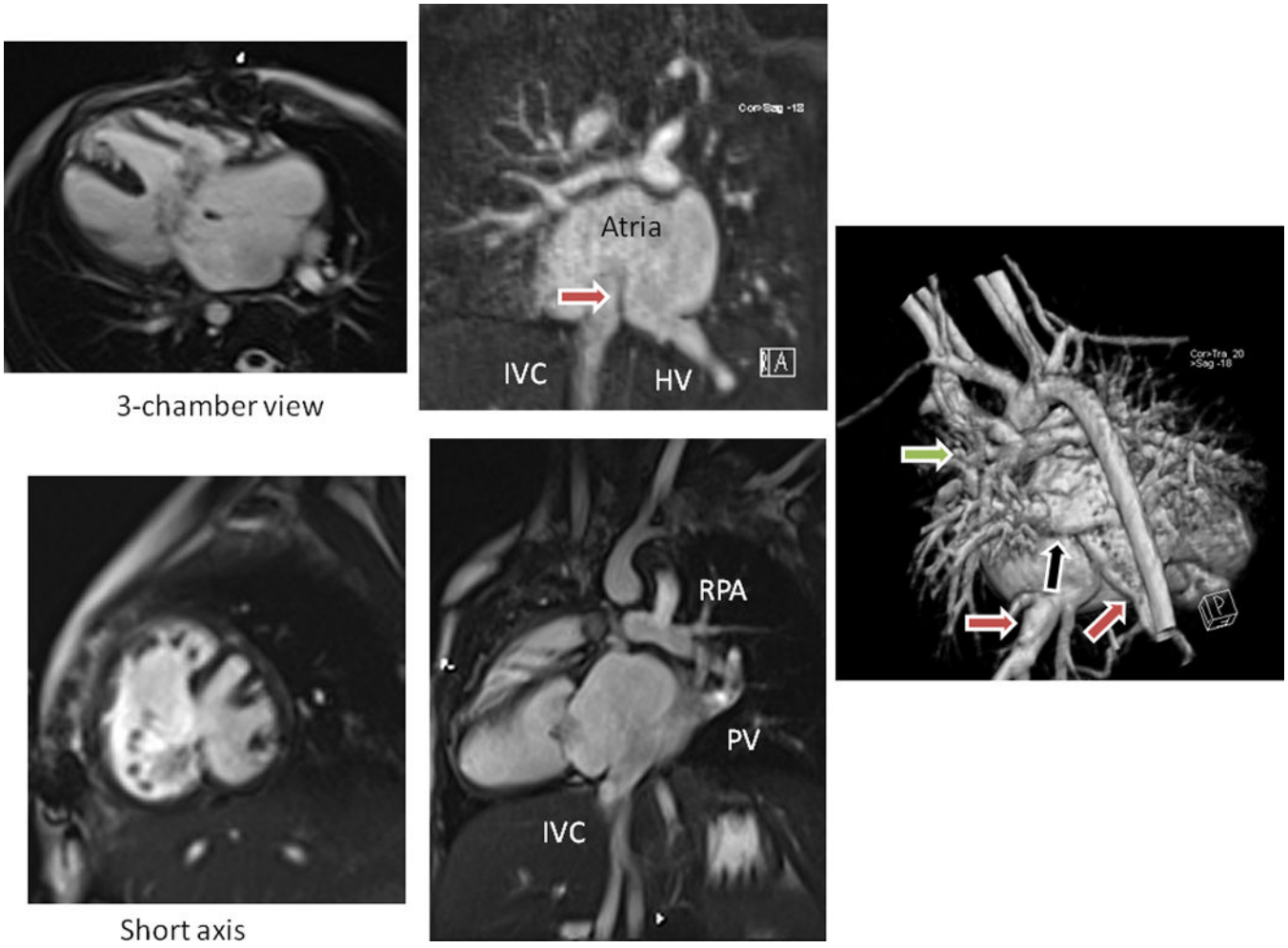

Figure 5.

Surgical planning in a standard Fontan patient - Clinical CMR for anatomy. Upper left is a cine of the 3-chamber view demonstrating the endocardial cushion defect and large atrial and ventricular septal defects, while lower left is a short axis view. Upper middle is a gadolinium image demonstrating the inferior vena cava (IVC) and left hepatic veins (HV) entering on different sided of the remnant of the atrial septum (arrow). Lower middle is an off-axis sagittal cine demonstrating the IVC, the pulmonary veins (PV), pulmonary venous confluence and right pulmonary artery (RPA). Note that the pathway from IVC to RPA for a Fontan connection would have the PV in the way. Right image is a 3D reconstruction from posterior demonstrating the IVC and HV (red arrows), the PV (black arrow) and the RPA, again noting the pathway from IVC and HV to the RPA with the PV in the way.

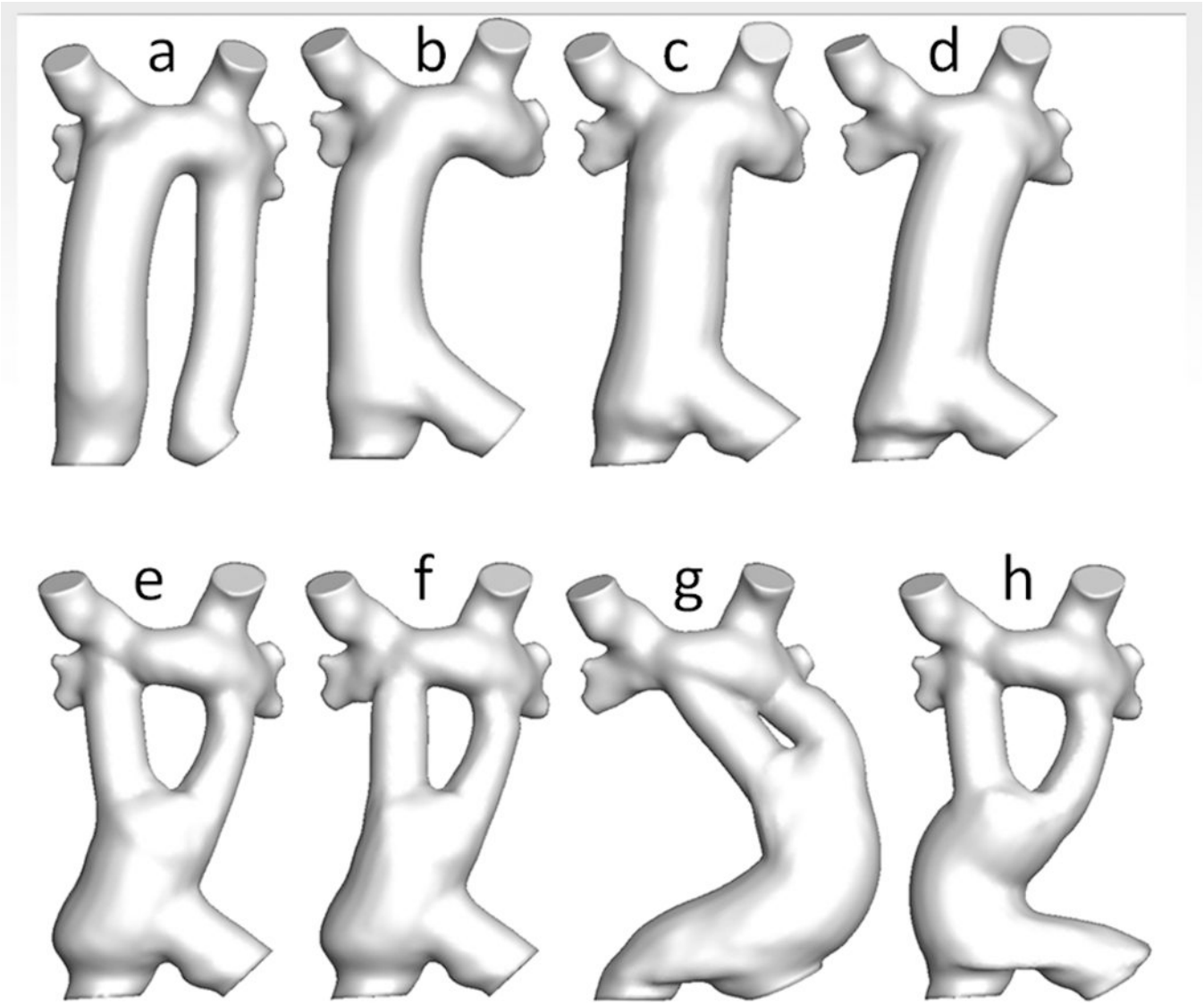

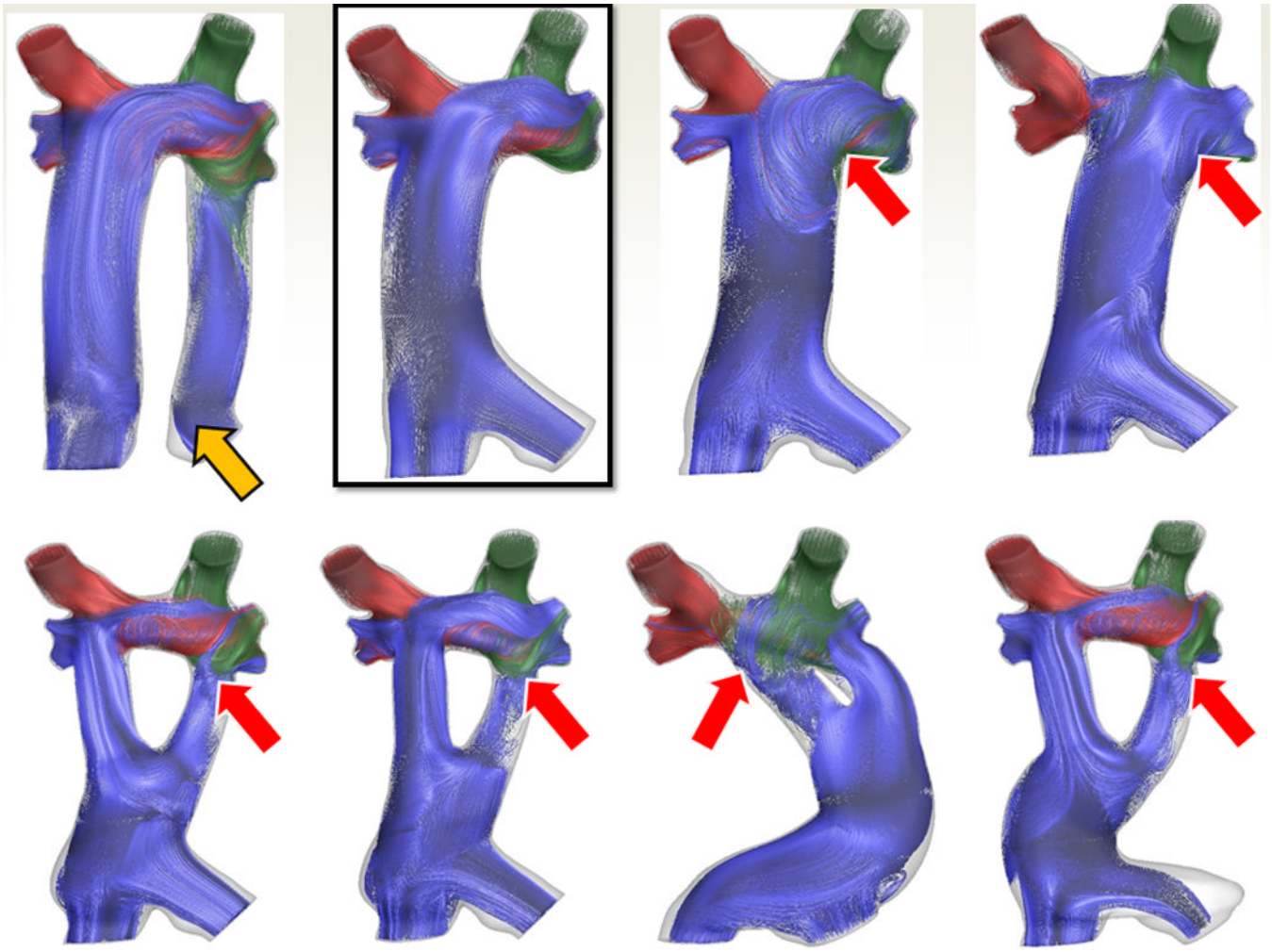

% Split to LPA of Hepatic Venous Flow

% Split to LPA of total PBF	a	b	c	d	e	f	g	h
55	30	33	69	76	N/A	21	92	4
68	53	47	78	92	16	57	100	14
80	69	70	94	100	52	85	100	54

Power Loss (mW)

% Split to LPA of total PBF	a	b	c	d	e	f	g	h
55	5.2	3	11.5	6	N/A	11.7	5.8	3
68	5.4	3.3	7.4	6.6	6.9	9.1	7.5	3.4
80	8.4	5.4	8.6	9	7.4	11.1	10.5	5.4

Figure 6.

Surgical planning in a standard Fontan patient – SP in patient from figure 5. (A) Eight virtual surgeries (a-e) with varying anatomic geometries. Note that “a” has a separate baffle for the left hepatic vein and lower virtual surgeries are all Y grafts; “g” courses long the left side of the heart. (B) Flow structures corresponding to the anatomies in B. Red arrows signify regions of turbulence while the yellow arrow demonstrates the flow too slow in the left hepatic baffle to sustain patency. Surgery B was chosen as optimal. (C) Charts of hepatic flow distribution (HFD) (top) and PL (bottom) for all the virtual surgeries at 3 flow splits to the left pulmonary artery (LPA); surgery “b” appears to have the best profile (green box). mW=milliwatts

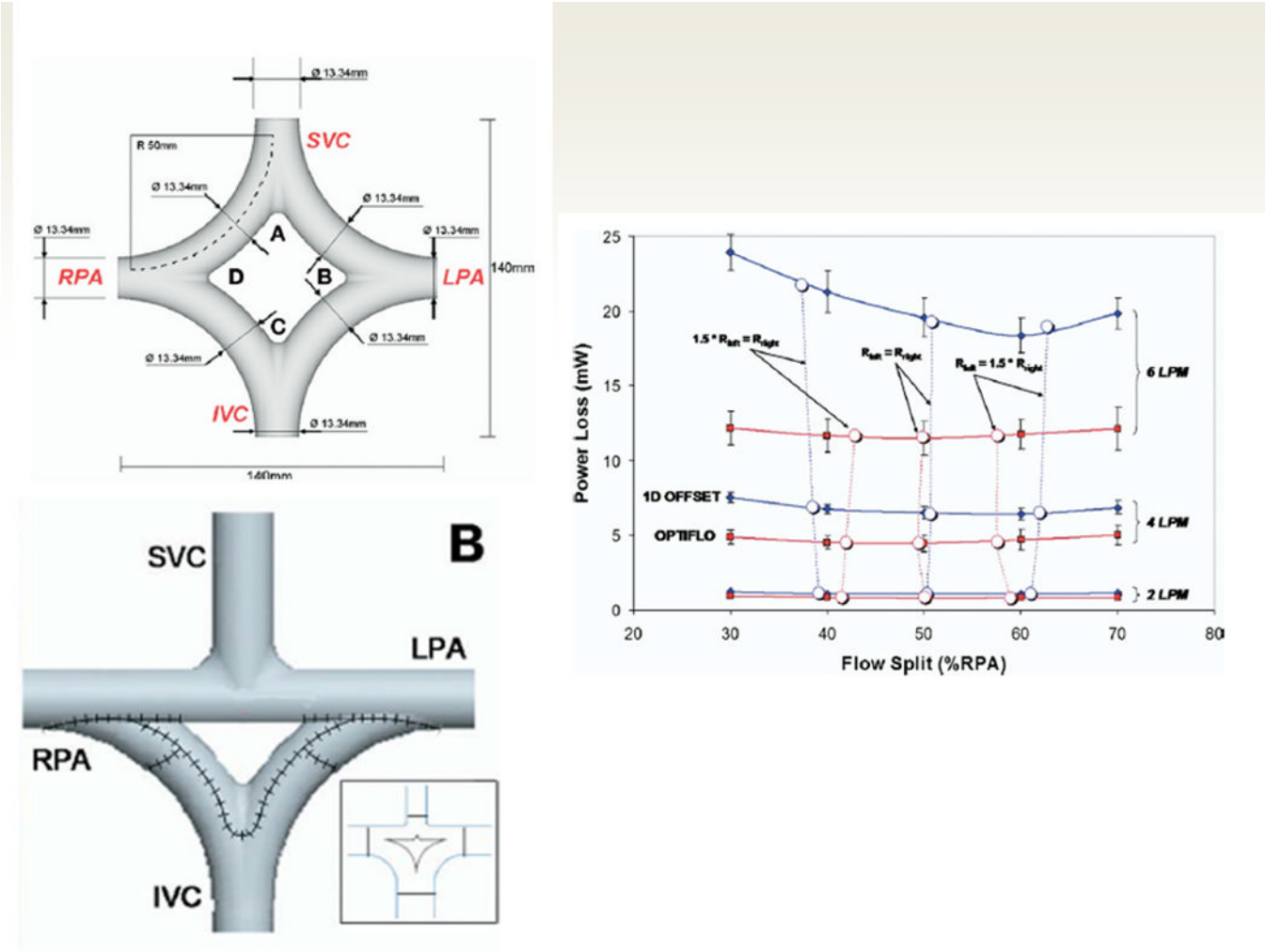

Figure 7.

The “Optiflow” design. Upper left panel demonstrates the diamond shape baffle configuration from the superior vena cava (SVC) and inferior vena cava (IVC) to the right (RPA) and left pulmonary arteries (LPA). The right panel demonstrates CFD modeling results with powerloss on the Y axis and flow split to the RPA on the X axis with the optiflow design performance on in red and the standard Fontan using a 1D offset (SVC and IVC baffle connection separated by 1 diameter) in blue. Note that at 2 liters per minute (LPM), the curves are nearly superimposed, however, at 4 and 6 LPM, the optiflow outperforms the standard Fontan (less power loss at any flow split to the RPA). The lower left panel shows a modification to the optiflow where the IVC baffle has a “Y” split (“Y” graft) but the SVC is not split (a triangle configuration), making it an easier Fontan to create. From Soerensen D, Pekkan K, de Zélicourt D, Parks J, Kanter K, Fogel M, Yoganathan AP. Introduction of a New Optimized Total Cavopulmonary Connection. *Annals of Thoracic Surgery*. 2007;83:2182–2190. With permission.

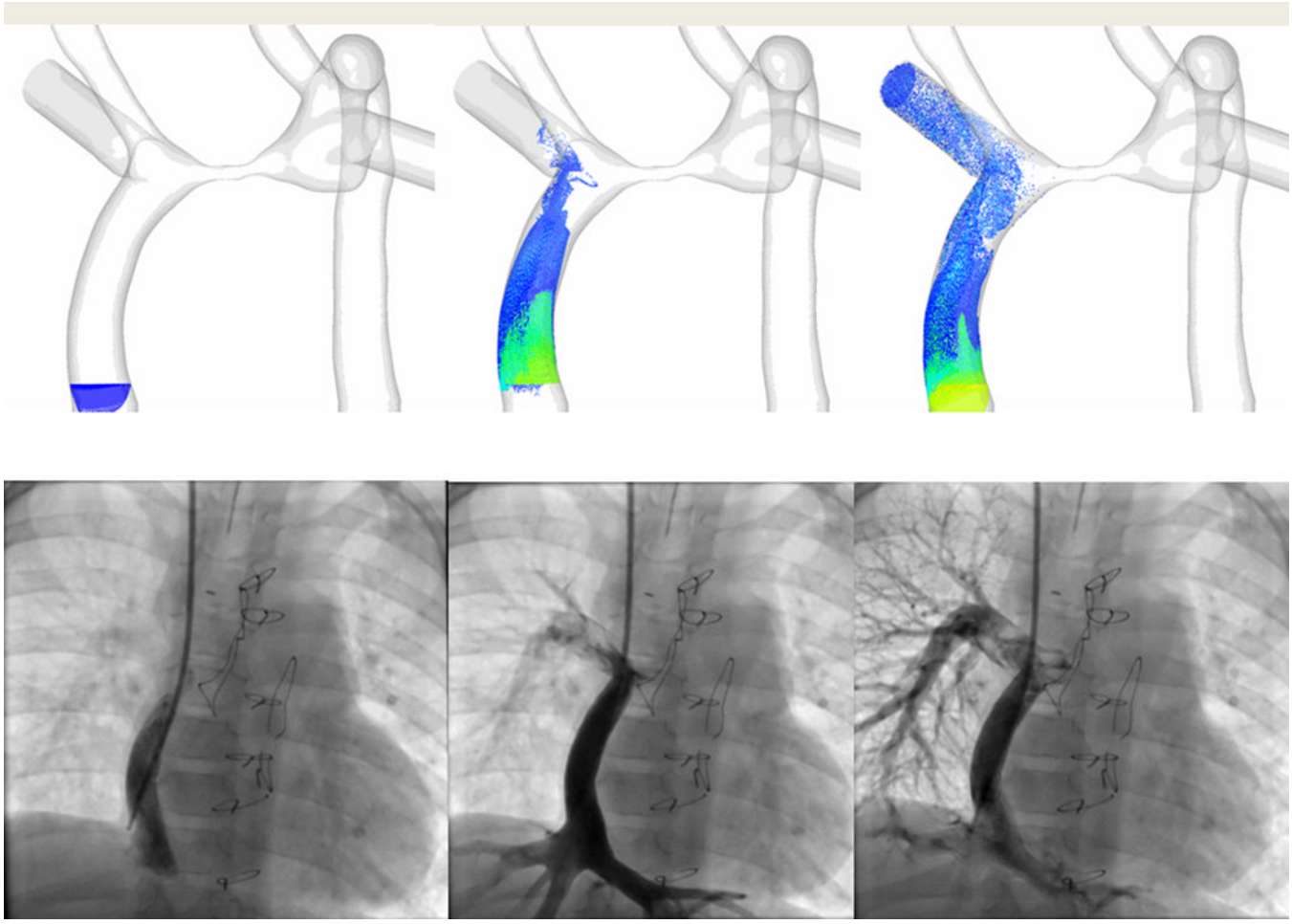

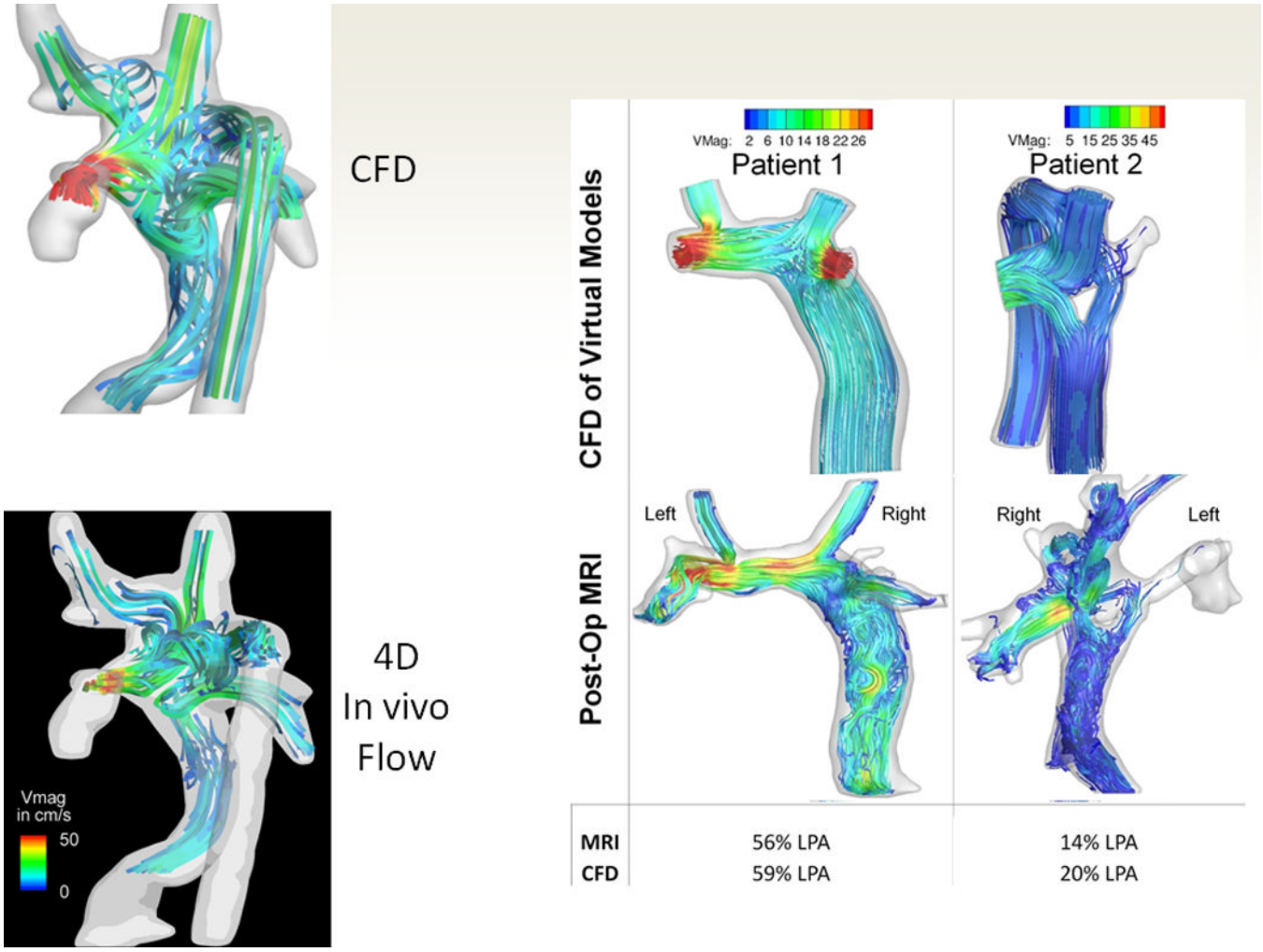

Figure 8.

Validation of the technique. (A). The 3 images on top are 3 phases (going in chronological order from left to right) of particle tracking with CFD in an SV patient with heterotaxy and interrupted IVC with azygous continuation to an LSVC after bilateral bidirectional Glenn and hepatic baffle. Particles are released in the hepatic baffle (left) and followed (middle and right). Bottom are 3 images of 3 phases (going in chronological order from left to right) from a catheterization in that same patient with the catheter at the base of the hepatic baffle. Note how the CFD is nearly identical to the angiography. (B) The top left is CFD modeling of the flow structure of a patient with heterotaxy and interrupted IVC with azygous continuation to an RSVC and the bottom left is the flow structure in the 4-dimensional flow data obtained in-vivo from that same patient. Note how identical the flow structures appear. The right panel is of 2 patients (one with a standard baffle in middle and Y graft on right) with single ventricle. The top 2 images is CFD modeling after SP and the bottom is the anatomy after surgery with the preoperative flows superimposed on the anatomy; again note how identical the flow structures appear. The bottom part of the panel is a table noting how close the MRI and CFD were to each other from calculated flow splits to the left pulmonary artery (LPA).